7772 *Macromolecules* **2009**, *42*, 7772–7780
DOI: 10.1021/ma901324b

Macromolecules
ARTICLE

Synthesis and Characterization of Biopolymer Composites from the Inside Out

Rosimar Rovira-Truitt,[†] Nitin Patil, Felissa Castillo, and Jeffery L. White*

Department of Chemistry Oklahoma State University, Stillwater, Oklahoma 74078. [†]Department of Chemistry, North Carolina State University.

Received June 19, 2009; Revised Manuscript Received August 21, 2009

ABSTRACT: The metal catalyzed ring-opening polymerization of D,L-lactide monomer inside the nanometer-sized channels of MCM-41 and SBA-15 hosts, creating an organic−inorganic hybrid polymeric material, is described. Detailed characterization of the polylactide/mesoporous silica organic−inorganic composite by multiple spectroscopic, microscopy, and calorimetric methods, as well as solvent extraction, reveals that the resulting in situ synthesized composite is unique relative to physical or solution-cast mixtures of polylactide and the mesoporous host. In this contribution, we focus on the incorporation of the stannous octanoate (Sn^{2+}) catalyst inside the mesoporous host channels prior to monomer introduction and subsequent polymerization and specifically target the differentiation of polymerization chemistry that occurs inside the host channels versus less desirable reactions on the exterior surface of the mesoporous host crystallites.

Introduction

Creating new hybrid materials that meet multiple constraints for performance in engineering, medical, and consumer applications while maintaining environmentally attractive waste disposal options requires novel synthesis routes. In this contribution, we demonstrate that known controlled architecture mesoporous hosts may be functionalized to produce an active catalyst for ring-opening polymerizations of biopolymer starting materials. Specifically, a Sn^{2+} catalyst is supported inside the channels of MCM-41[1] or SBA-15[2] to generate a spatially unique ring-opening catalyst for the conversion of D,L-lactide to poly(D,L)lactide, also known as poly(D,L-lactic acid) (PDLLA). The resulting polymer forms inside the host channels and ultimately is extruded out of the channel as the molecular weight increases. In this way, a biodegradable and biocompatible organic/inorganic nanocomposite is formed in situ. However, as the polymer chain originates from inside the host channels, they cannot easily segregate from the inorganic component, thereby ensuring intimate contact. To demonstrate reproducible synthesis of the polymer originating from within the host, we present multiple experimental results from solid-state NMR, calorimetry, microscopy, nitrogen adsorption, X-ray diffraction, and wet chemical methods, indicating that important steps in the chemistry, both for catalyst synthesis and D,L-lactide polymerization, occur inside the host channels versus outside on the crystallite surfaces.

Recent activity in the synthesis and preparation of organic−inorganic composites or nanocomposites, as they are most often termed, has expanded the materials science field.[3] Natural layered or pillared clays,[4−6] carbon nanotubes,[7−9] carbon, and natural fibers[10−12] have replaced more traditional materials and methods, like physical mixing of fumed silica[13] or carbon black as constituents that when placed in polymeric hosts at low volume or weight percents significantly modify the final physical or mechanical properties. Success in these areas depends significantly on the degree to which the inorganic component is homogeneously distributed in the polymeric matrix and most commmonly involves clays where exfoliation is the key step. In more recent work, synthetic micro- and meso-crystalline silicates and aluminosilicates, that is, zeolitic and crystalline mesoporous MCM-41 materials, have garnered attention.[14] The microcrystalline channels of zeolite materials, whose cross-sectional channel dimensions typically are less than 1 nm, can pose problems for materials synthesis since many polymers and even their respective monomers encounter diffusion barriers inside the crystalline void volume, although in a recent case, high pore loadings were achieved.[15] Typically, approaches to date can be categorized as either physical mixing methods, where the polymer (at its final molecular wieght) and inorganic reinforcing agent of choice are mixed together as a function of temperature or solvent, or by introducing the monomer and completing the polymerization in the presence of the inorganic reinforcing agent. The latter approach has been particularly successful for petroleum-based and olefin polymers.[16−21]

Polymers generated from naturally produced monomers, for example, polylactide, are biocompatible and biodegradable, and could have an increased impact in consumer materials or health field applications given a larger, more flexible range of physical properties. A relatively fewer number of reports have targeted enhanced properties of polylactides through composite formation.[22,23] Here, we discuss an in situ approach using the D,L-lactide monomer and a modified MCM-41 or SBA-15 catalyst that supports the ring-opening Sn^{2+} catalyst. In contrast to a previous report in which an acid functionalized ring-opening mechanism for polymerization of a valerolactone monomer was proposed,[22] we find through additional experiments utilizing Al-functionalized MCM and SBA hosts that this does not occur for lactide monomers. The Sn complex (stannous octoate) must be incorporated into the mesoporous host for D,L-lactide polymerization to occur. Here we also demonstrate that a material formed by the simple mixing of the inorganic matrix and the organic poly(D,L-lactide) polymer is not equivalent at the polymer/surface interface to the new material generated by the in situ polymerization approach. In this contribution we discuss the details of host synthesis, active catalyst preparation, and polymerization of D,L-lactide with our supported catalyst approach to create the

*Corresponding author. E-mail: jeff.white@okstate.edu.

 Published on Web 09/04/2009

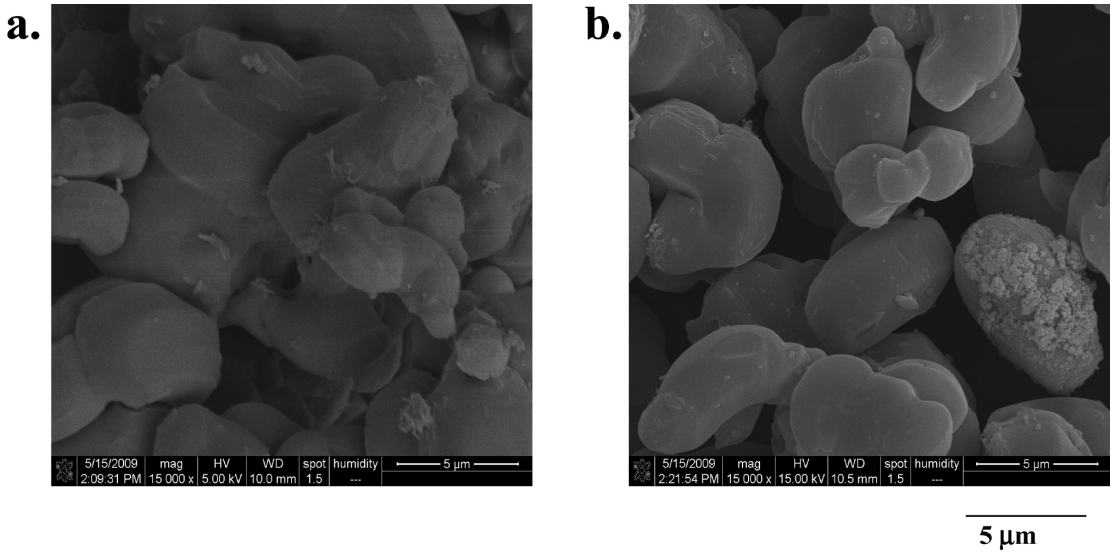

Figure 1. (a) SEM image of pure MCM-41. (b) SEM image of MCM-41 containing the supported $Sn(Oct)_2$ ring-opening catalyst, specifically, the Sn/MCM-41_2 sample.

final biopolymer composite material, as well as subsequent molecular and physical characterization results for that composite with *specific emphasis on polymer that is actually made within the interior of the mesoporous host*.

Experimental Section

Materials. D,L-Lactide (97%) was obtained from Alfa Aesar. Tin(II) 2-ethylhexanoate ($Sn(Oct)_2$; 95%) and 1-dodecanol (98%) were purchased from Sigma-Aldrich. All organic solvents were obtained from Pharmco-AAPER.

Characterization. Molecular weight (M_w) analyses were performed on a Series 1100 HP Size Exclusion Chromatography (SEC) instrument with a polystyrene (PS) column. Glass transition temperatures T_g were measured using a 5°/min ramp on a Q2000 Thermal Analysis (TA) differential scanning calorimetry (DSC) instrument. Elemental analysis of the final catalyst formulations was performed by Galbraith Laboratories using inductively coupled plasma−atomic emission spectroscopy (ICP-AES). X-ray diffraction (XRD) patterns were obtained on a Bruker AXS D-8 Avance X-ray powder diffractometer using copper K_α radiation. Analysis was completed using a search/match program and the PDF-2 database of the International Center for Diffraction Data. Specific surface area BET measurements were performed on a Quantachrome Nova 1200 Surface Area Analyzer using nitrogen adsorption. Thermal gravimetric analysis (TGA) was performed on a Shimadzu model 50 instrument. Scanning electron microscopy (SEM) and transmission electron microscopy (TEM) data were obtained using FEI Quanta 600 ESEM and JEOL JEM-2100 microscopes, respectively. Solid-state NMR experiments were performed on a Bruker DSX spectrometer operating at 7 T, which corresponds to a ^1H Larmor frequency of 300 MHz. Magic-angle sample spinning (MAS) speeds ranged from 4 to 10 kHz, depending on the specific experiment. The ^1H $T_{1\rho}$ experiments were carried out via indirect detection of the directly attached carbons using cross-polarization.[24] Carbon Bloch decay (^{13}C single-pulse) experiments consisted of a 90° pulse with a delay time of 20 s. The ^1H to ^{13}C cross-polarization (CP) pulse sequence consisted of a 3.7 μs 90° pulse on the proton channel followed by a 1-ms contact pulse for heteronuclear polarization transfer.[25] All carbon NMR data were acquired with proton decoupling at radio frequency field strengths equal to 70 kHz.

Sn Supported Mesoporous Catalyst (Sn/MCM-41). MCM-41 was synthesized following the procedure described by Zhao.[26] For a typical synthesis, 0.800 g of NaOH, 59.994 g of deionized water, 2.523 g of cetyltrimethylammonium bromide (CTAB), and 2.403 g of SiO_2 were thoroughly mixed and aged in a Parr acid digestion bomb for three days at 100 °C. The material was filtered and washed with excess deionized water and calcined at 550 °C for 10 h using a 1 °C/min ramp. The supported catalyst was prepared by stirring stannous octoate ($Sn(Oct)_2$) with the calcined MCM-41 material at different Sn/Si ratios for 3 h. Excess stannous octoate was filtered and the remaining material was rinsed with 2 L of hexanes and dried overnight. Throughout the remainder of the text, we denote each supported catalyst by the relative amounts of Sn and Si, for example, Sn/MCM-41_2 indicates a catalyst with a calculated Sn/Si atom ratio of 2 based on the starting ingredient concentrations.

Poly(D,L-Lactide)/Sn/MCM-41 Hybrids. Pure poly(D,L-lactide) was synthesized following established methods.[27] The monomer was recrystallized with toluene and kept under vacuum. The monomer, catalyst, and dodecanol co-initiator were placed in a round-bottom flask equipped with a stir bar, and the reaction was carried out for 2 h at 175 °C in an oil bath. Excess monomer was removed by dichloromethane addition and precipitating in methanol. The molar composition was 1 mol D,L-lactide to 7.11×10^{-5} mol $Sn(Oct)_2$ to 3.87×10^{-5} mol of 1-dodecanol. The organic−inorganic hybrid was obtained by stirring the monomer, Sn/MCM-41 supported catalyst, and 1-dodecanol for 2 h at 175 °C. The molar gel composition was 1 mol D,L-lactide to 7.11×10^{-3} mol $Sn(Oct)_2$ to 3.87×10^{-3} mol of 1-dodecanol. Washes of the hybrid material were obtained by rinsing with 15−30 mL of dichloromethane. A physical mixture of the Sn/MCM-41 catalyst and the pure PDLLA (control sample; $M_w = 50000$) was prepared by stirring the two together for 2 h at room temperature. The resulting blend was dried overnight.

Results and Discussion

Mesoporous Host with Supported Sn Catalyst. As-synthesized MCM-41 exhibited the well-defined X-ray powder pattern previously reported, with four characteristic (including the 100) reflections between $2 < 2\theta < 6$ and BET surface areas in excess of 1000 m^2/g.[1,26] Solid state ^{29}Si MAS and ^1H to ^{29}Si CP/MAS NMR experiments revealed characteristic chemical shifts for Si atoms at −92, −101, and −110 ppm, corresponding to Si atoms in Q^2, Q^3, and Q^4 lattice positions, respectively.[28,29]

Figure 1a shows SEM images for the pure MCM-41 typical of the type used as a basis for further modification

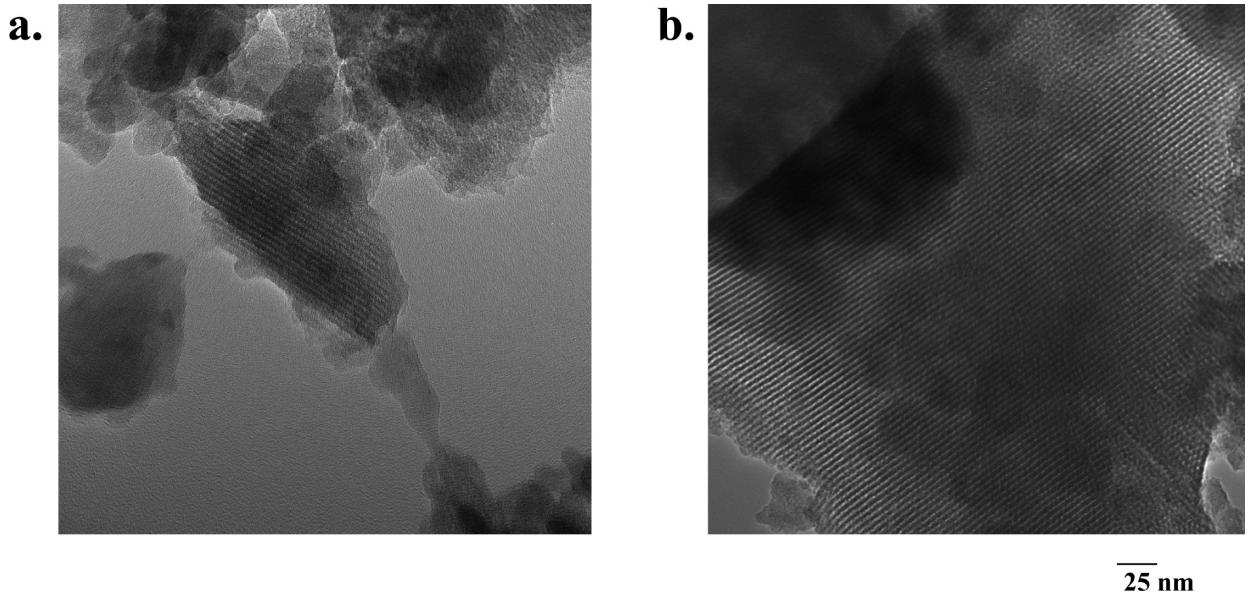

Figure 2. TEM images of (a) pure MCM-41 and of (b) the Sn/MCM-41_2 catalyst.

to make the final composite; average particle dimensions are about 5 μm. While a majority of recent work has focused on making smaller particle dimensions, we favor the larger crystallites for this initial investigation since the interior volume to exterior surface area ratio is maximized. Incorporation of the $Sn(Oct)_2$ into the MCM-41 to create the supported ring-opening catalyst, followed by washing to remove excess Sn catalyst, did not alter the SEM data as shown in Figure 1b. Indeed, TEM reveals that the one-dimensional crystalline channel structure of MCM-41 is preserved after the final $Sn(Oct)_2$/MCM-41 composite catalyst is made, as observed by comparing Figure 2b to Figure 2a.

The microscopy data indicates that the catalyst morphology and channel structure were not altered by preparation of the $Sn(Oct)_2$ modified catalyst. However, BET surface area measurements showed a decrease in surface area from > 1000 m^2/g for the starting MCM-41 material to 400 m^2/g for the Sn/MCM-41 catalysts, independent of whether the initial Sn/Si atomic ratio in the synthesis mixture ranged from a value of 2−35. We verified the Sn concentrations in several Sn/MCM-41 catalyst formulations via elemental analysis, as summarized in Table 1.

The results in Table 1 indicate that the background level of Sn as an impurity in the synthesis of pure MCM-41 is very low and as confirmed by control experiments, too low to effect any polymerization of the D,L-lactide monomer. Most importantly, one observes that varying the initial amount of Sn in the synthesis by over an order of magnitude (2−35 Sn/Si ratio) has relatively little effect on how much Sn survives with the MCM host following the synthesis and subsequent washings. Obviously, our initial Sn/Si compositions represent significant Sn excess. This is in agreement with the BET surface area measurements, indicating that the stable incorporation of $Sn(Oct)_2$ in MCM-41 reaches an upper limit. We obtained very similar results from elemental and surface area measurements in separate catalyst formulations where MCM-41 and SBA-15 that each contained framework Al atoms were used as the inorganic host material. While detailed experiments on the Al-containing MCM-41 and Al-containing SBA-15 materials are not the subject of this contribution, the fact that the presence of Al in the framework does not alter the amount of $Sn(Oct)_2$ that can be incorporated in the mesoporous host

Table 1. Comparison of Sn Concentrations in Several Initial Synthesis Mixtures to that in the Final Catalyst[a]

materials	Si (wt %)	Sn (wt %)	Sn/Si (calcd)	Sn/Si (exp)
MCM-41	28.4	< 371 ppm		
Sn/MCM-41_35.4	21.9	27.0	35.4	0.291
Sn/MCM-41_10.9	27.1	16.4	10.9	0.143
Sn/MCM-41_2	26.7	19.6	2.0	0.173
washed PDLLA_Sn/ MCM-41_35.4	17.6	19.3	0.291	0.259

[a] The data in the column Sn/Si (exp) is from elemental analysis on the final washed catalyst.

relative to purely siliceous hosts indicates that a charged host framework is not required to support the $Sn(Oct)_2$ (vide infra).

Figure 3 summarizes results from quantitative ^{13}C Bloch decay single-pulse MAS NMR experiments. The spectrum of the pure $Sn(Oct)_2$ (a viscous liquid) is shown for reference in 3a. Even with excessive washings using 1−2 L of solvent, a fixed amount of the $Sn(Oct)_2$ catalyst remains in the MCM-41 host, and the differential peak intensities and widths for similar carbons in the octanoate ligands indicates that the complex has adopted a constrained geometry, that is, the $Sn(Oct)_2$ resides in a specific location in the channels of the MCM-41. This is particularly evident when comparing Figure 3b, the supported but unwashed catalyst complex, with Figure 3d or e. If the spectra for the catalyst complex are generated via cross-polarization from ^1Hs in the ligand to ^{13}C nuclei in the ligand, this requires an immobile, constrained catalyst for the requisite dipolar interactions to persist. The ^1H to ^{13}C CP/MAS data in Figure 4 show that indeed the octanoate ligands in the washed Sn/MCM-41 catalyst meet this requirement, and strong signals are obtained for contact times as short as 100 μs. Comparing the quantitative Bloch decay spectrum in Figure 4a to the 1 ms contact time CP experiment in Figure 4b indicates, by virtue of the similar peak intensities and chemical shifts, that the CP/MAS data does not reflect a minor fractional component of the catalyst complex but is representative of the majority of the supported catalyst. One key difference is that the carbonyl signal centered near 180−185 ppm exhibits a larger line width in the CP/MAS result of Figure 4b, and its center

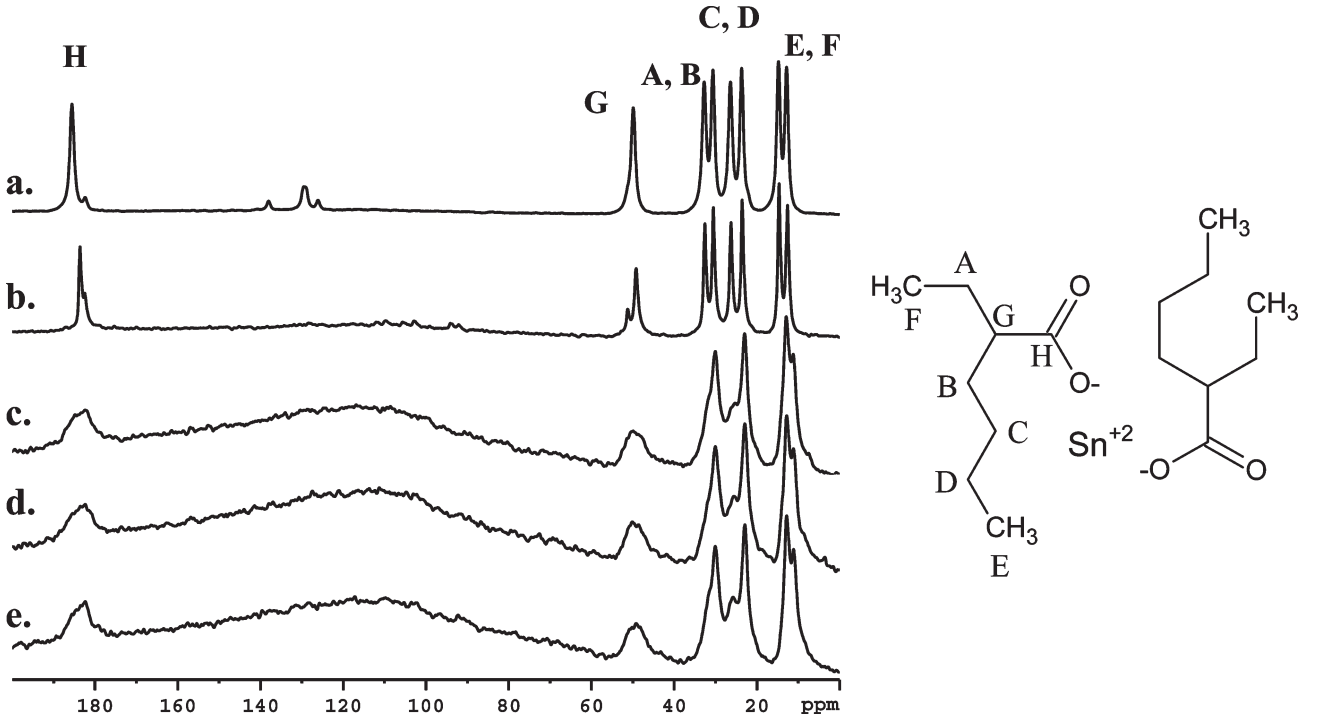

Figure 3. ^{13}C MAS NMR spectra of (a) pure $Sn(Oct)_2$ prior to catalyst formulation; and various Sn/MCM-41_35.4 catalysts following the indicated solvent washings: (b) unwashed, (c) 600 mL wash, (d) 1200 mL wash, and (e) 2000 mL wash. Spectra were acquired with 70 kHz ^1H decoupling r.f. field strengths during acquisition, and with MAS speeds = 6 kHz . The broad central hump in c−e is a residual carbon background signal from the probe.

of mass is shifted downfield by 2−3 ppm relative to Figure 4a, suggesting that the CP/MAS experiment is emphasizing that fraction of the catalyst complex ligands that interact most strongly with the host surface.

The combined results from the BET, microscopy, elemental, and solid-state NMR analyses indicate that the $Sn(Oct)_2$ complex is supported inside the MCM-41 channels, which is critical to our original goal of generating poly(D,L-lactide) from the monomer *inside* the host channels. As mentioned previously, the purely siliceous MCM-41 is a charge neutral framework, and therefore, one can ask if and how the $Sn(Oct)_2$ interacts with the channel walls of the host to form a stable catalyst for the subsequent ring-opening polymerization. Recall that dodecanol is added simultaneously with the monomer in the polymerization step but is not present when making the supported $Sn(Oct)_2$/MCM-41 catalysts described in the preceding data. Figure 5 shows possible schemes based on hydrogen bonding or dipole−dipole interactions between MCM-41 surface hydroxyls and the Sn^{2+} catalyst complex. There is experimental evidence for the scheme in Figure 5a; a 183 ppm peak is detected in the liquid ^{13}C NMR spectrum of the solvent washes, characteristic of the 2-ethylhexanoic acid byproduct of the catalyst complex formation.

Poly(D,L-lactide)/MCM-41 Composites. Kageyama and co-workers reported the polymerization of ε-caprolactone and γ-valerolactone using an Al-MCM-41 catalyst and butanol co-initiator.[30] The reaction was carried out at 50 °C under nitrogen atmosphere, and presumably, the Al-MCM-41 acted as a Lewis acid in the initiation step. To generate proper control data, we explored if aluminum-containing mesoporous materials or their purely silicious analogues, each in the presence of an alcohol cocatalyst, could polymerize D,L-lactide. Amorphous SiO_2 as well as crystalline MCM-41, Al-MCM-41, SBA-15, and Al-SBA-15 were each stirred together with the monomer and co-initiator 1-dodecanol for 2 h at 175 °C in an oil bath. Carbon NMR

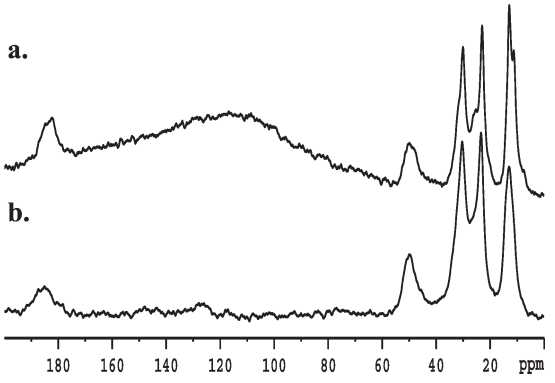

Figure 4. Comparison of ^{13}C results for the same Sn/MCM-41_35.4 catalyst sample in Figure 3e: (a) Bloch decay/MAS spectrum; (b) CP/MAS spectrum acquired with a 1 ms polarization transfer time.

experiments indicated that polymerization did not occur, consistent with the physical characteristics of the final product mixture. These combined results confirm that the supported $Sn(Oct)_2$ complex is a required component for the active mesoporous D,L-lactide polymerization catalyst.

Two catalysts with different as-prepared Sn concentrations, that is, Sn/Si = 2 and Sn/Si = 35, were evaluated for their D,L-lactide polymerization activity according to the procedure described in the Experimental Section. As previously mentioned in Table 1 and the supporting discussions, these catalysts are denoted as Sn/MCM-41_2 and Sn/MCM-41_35, respectively. Figure 6 shows TGA results for all materials used at each stage of catalyst synthesis, as well as that for a final composite made using a Sn/MCM-41_2 catalyst. Compared to the pure MCM-41, we observe that the water adsorption capacity after $Sn(Oct)_2$ incorporation is reduced by a factor of 2, indicating that the catalyst complex is incorporated inside the MCM channels, as previously suggested, and in agreement with previous BET results for

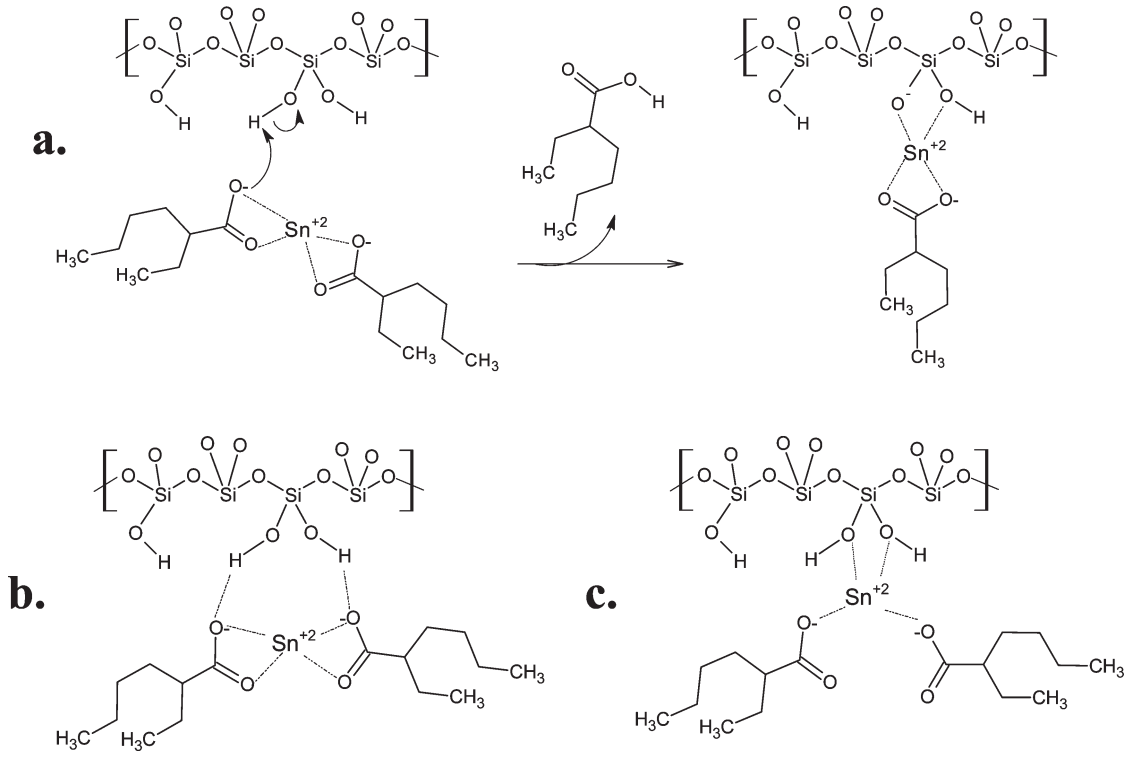

Figure 5. Reactions/structures depicting possible modes of interaction between the $Sn(Oct)_2$ complex and the interior walls of the MCM-41 channels. (a) Proton transfer to yield a free carboxylic acid ligand and the tethered Sn catalyst complex; (b) hydrogen bonding association, which could be either geminal (shown) or vicinal hydroxyl groups on the surface; (c) dipole−dipole interaction between the metal atom and surface oxygens, which could also involve nonprotonated bridging oxygens from the surface (not shown).

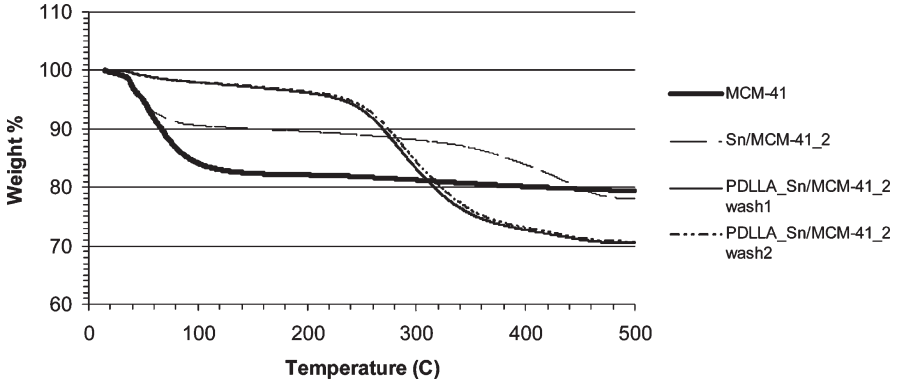

Figure 6. TGA results for pure MCM-41, Sn/MCM-41_2, a PDLLA_Sn/MCM-41_2 composite washed with 15 mL CH_2Cl_2 (wash 1) and PDLLA_Sn/MCM-41_2 washed with 30 mL CH_2Cl_2 (wash 2).

the catalyst. More importantly, water adsorption within the MCM channels is precluded in the polymer composite materials, clearly demonstrating that the polymer which is being made, and removed by thermal decomposition in the TGA experiment, is polymer which originates inside the channels of the Sn/MCM-41_2 catalyst. All catalyst and composite samples were prepared in the presence of ambient moisture, that is, there were no special sample handling or inert atmosphere preparation steps to preclude exposure to moisture.

The TGA results for both of the washed polymer composite samples in Figure 6 agree with further reductions in accessible surface area relative to the pure MCM-41 or the Sn/MCM-41 catalyst complex. BET measurements on the polymer composite yielded, on average, 25 m^2/g surface area, which is lower than that of the Sn/MCM-41 catalyst (400 m^2/g) but still larger than the 5 m^2/g measured on pure poly(D,L-lactide) prepared via conventional routes. TEM data for the polymer composites revealed that MCM-41 channel integrity was unchanged following polymerization; Figure 7 shows the characteristic worm-like mesopores with 4 nm pore opening.

While the TGA and BET experiments are bulk measurements, Figure 8 shows solid-state CP/MAS spectra for the polymer composites, as well as results from an important control experiment. Solid-state NMR can provide local length scale information compared to TGA or BET experiments. The spectrum for the as-prepared composite, but prior to solvent washing to remove any extractable polymer components, is shown in Figure 8a. Except for the increased linewidths, the result looks in every way similar to the CP/MAS spectrum for bulk amorphous poly(D,L-lactide) prepared via conventional methods. Note that all three chemical shifts for chemical moeties in the polymer are different by

2−6 ppm than their respective peak in the D,L-lactide monomer, so polymerization has definitely occurred. In other words, simply adsorbing monomer in the host materials cannot generate the spectra shown in Figure 8. After washing with 600 mL of CH_2Cl_2, the spectrum in Figure 8b is obtained in which we see the clear appearance of broad downfield shoulders on both the polymer C=O and CH_3 signals.

Vertical expansion of the spectrum in Figure 8a (not shown) reveals that these features are also present in the unwashed sample, but at a much lower fraction of the total polymer chains. The broad downfield shoulder on the carbonyl peak (170−185 ppm) of the washed polymer composite (Figure 8b) indicates that the polymer has significant hydrogen bonding contacts with hydroxyl groups in the channels of the MCM-41 host. Further, it is known that pendant methyl groups are excellent reporters of conformational inequivalence in polymer chains, and the strong shoulder at 21 ppm on the 18 ppm CH_3 peak supports this assignment. The solid-state CP/MAS NMR results indicate that the polymer chain inside the host channels hydrogen bonds with the MCM-41 hydroxyl groups. ^{1}H rotating frame spin−lattice relaxation rate time constants $T_{1\rho H}$ decreased by a factor of 4 (48 to 12 ms) in going from pure poly(D,L-lactide) to the washed polymer composite sample of Figure 8b. By comparison, Figure 8c and d show results for identical experiments to that in Figure 8a and b, except

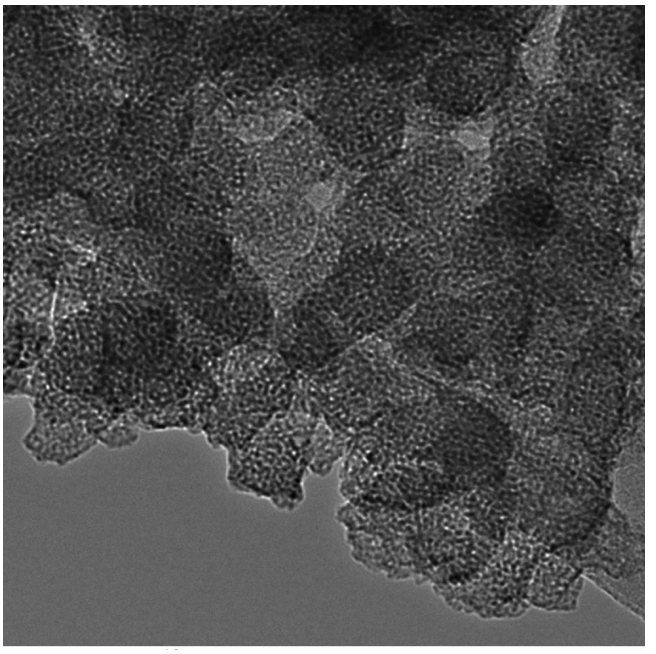

Figure 7. TEM of the washed PDLLA_Sn/MCM-41 composite.

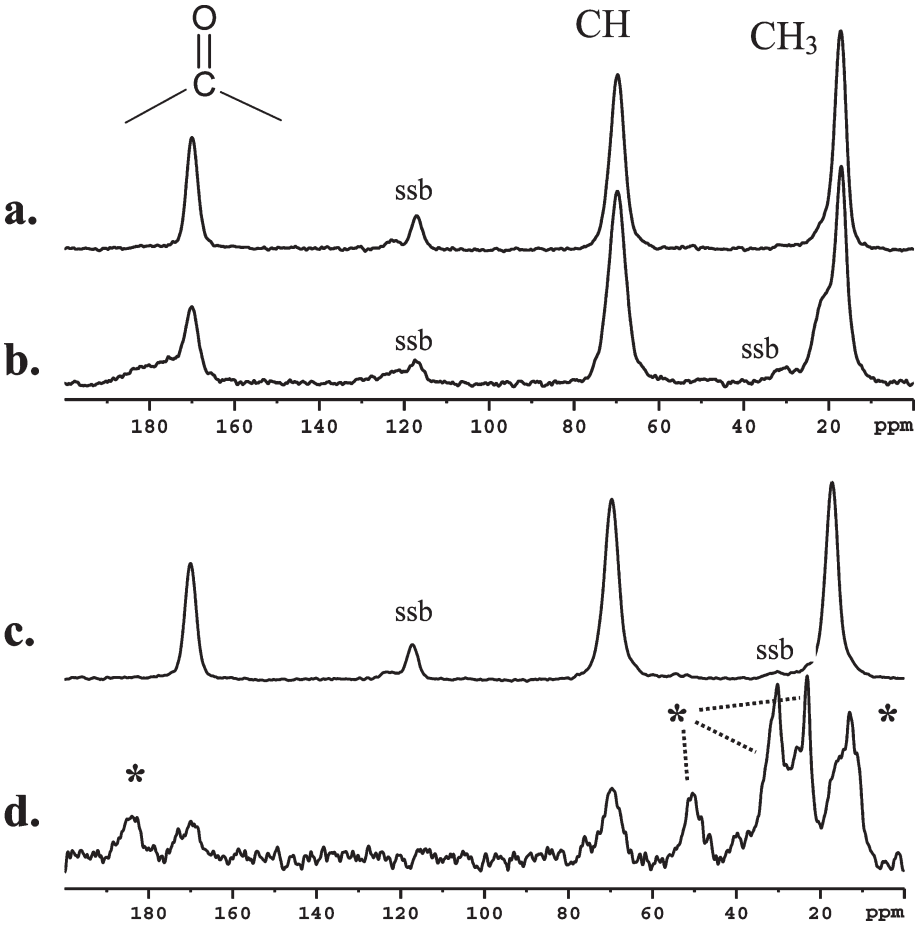

Figure 8. ^{13}C CP/MAS NMR spectra of PDLLA_Sn/MCM-41_35.4 polymer composites: (a) the composite as prepared in situ using the procedure outlined in the text, but prior to washing; (b) same sample as in (a) after washing with 600 mL of CH_2Cl_2; (c) a blend of poly(D,L-lactide) and the Sn/MCM-41 catalyst complex prepared as described in the Experimental Section, prior to washing; (d) same sample as in (c) after washing. Spectra were acquired with 70 kHz ^{1}H decoupling r.f. field strengths during acquisition. In (d), * denotes signals from the ligands of the supported Sn complex. Spinning sidebands are indicated by "ssb".

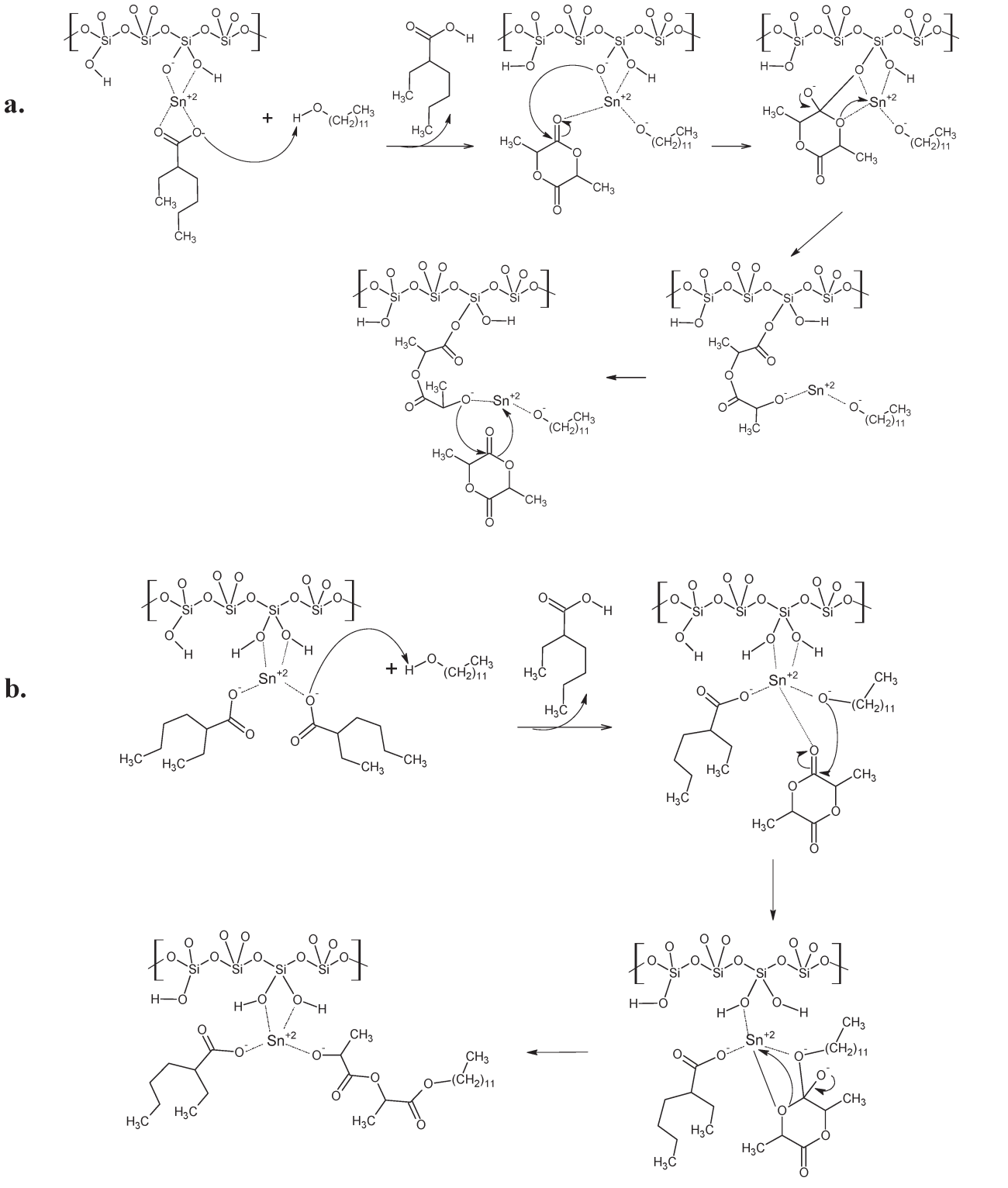

Figure 9. Scheme depicting the introduction and subsequent reaction of 1-dodecanol and D,L-lactide monomer into the channels of Sn/MCM-41: (a) via the proposed ion-exchanged supported catalyst and (b) via the proposed catalyst with a weak bond association between the Sn atom and the surface hydroxyl groups.

that the sample is a blend of poly(D,L-lactide) and the Sn/MCM-41 composite catalyst. In other words, the polymer itself was not generated from the monomer in situ in the presence of the catalyst host complex, but mixed with the catalyst complex at the same temperature (175 °C) that the polymerizations were done for the in situ prepared composites and then cooled. The as-prepared unwashed spectrum in Figure 8c looks almost identical to that in Figure 8a. However, following the same 600 mL CH_2Cl_2 wash procedure for this blend as was used to generate the spectrum in Figure 8b, the spectrum in Figure 8d shows that essentially all of the poly(D,L-lactide) is completely removed from the MCM-41 host. Indeed, the strongest signals in the spectrum for the washed blend sample come from the octanoate ligands of the supported Sn catalyst, denoted by asterisks in the figure.

Molecular weight analysis of the resulting poly(D,L-lactide)/MCM-41 composites by GPC is problematic due to relatively high MCM-41 composition in the washed samples. As stated earlier in the manuscript, our emphasis on identifying and characterizing the polymer that originates and remains within the host channels after a strong solvent extraction step requires a higher mass fraction of the host than one might choose to employ for applied work. On average, the GPC results indicate that the polymer chains have approximately one-fifth the molar mass of bulk, as-synthesized pure polymer (10000 vs 50000). However, one should regard molecular weight data by GPC for these composites with some skepticism, because the hydrodynamic properties of the washed polymer composites are much different than that of bulk polymer chains. The use of relatively high concentrations of Sn-catalyst complex in this study, as needed to adequately characterize interior-channel surface interactions, results in lower polymer molecular weights.

Based on the evidence presented above, we propose a mechanism for how polymerization occurs within the channels of the MCM-41 host in which the Sn^{2+} catalyst is supported. As discussed earlier in Figure 5, we cannot specify the exact structure of the supported Sn catalyst complex, but two reasonable possibilities exist as a starting point for polymerization. Figure 9 shows the same ring-opening mechanism of the D,L-lactide monomer in the presence of the dodecanol initiator but starting from two different Sn complex structures. Proposed mechanisms for the polymerization of lactones using stannous octanoate catalysts have been published in the literature and suggest a coordination−insertion mechanism.[31,32] Irrespective of whether the reaction initiates as shown in Figure 9a or 9b, the main barrier to propagation and generation of higher molecular weight polymer ($> M_w = 10000$) is diffusion of monomer to the active catalyst site in the presence of a growing polymer chain within the limited channel dimensions. Larger channels hosts may be preferable, and we are currently pursuing detailed experiments in this direction.

In the absence of very copious amounts of solvent used in the washing of the Sn-supported catalyst, prior to polymerization, one might expect external surface contributions. However, it is known that MCM-41, unlike amorphous silica, has hydroxyl groups that are all equally accessible to small molecule sorbents. One also expects by virtue of the curved walls of the 4 nm channels, the average effective hydroxyl group density is higher inside the channels than on the outer surface, even for a constant 3−4 hydroxyl groups per square nanometer. With the exhaustive washing to prepare the supported Sn catalysts, it is simply most probable that the initial condition will correspond to a case where the monomer will begin chemistry inside the MCM-41 channels. This is consistent with a limit reached on how much Sn remains in the catalyst based on the elemental analysis data and also with the fact that half of the MCM-41's water sorption capacity is eliminated upon formation of the supported catalyst, as shown by the TGA Figure 6. Further, based on comparisons to well-known nonporous bead materials, a reasonable comparison for an external surface area measurement of the MCM crystallites, 400 m^2/g is much too high for the external surface of particles with average 5 μm size. Typically, nonporous surfaces with an average 5 μm size would be expected to exhibit surface areas in the range 2−5 m^2/g, fully 2 orders of magnitude lower than what we measure. Even by considering the surface roughness of the MCM-41 particle, the measured value is still far too high to associate with external surface contributions.

Conclusions

A stable ring-opening polymerization catalyst can be prepared within the channels of the mesoporous hosts MCM-41 and SBA-15. Using $Sn(Oct)_2$ catalyst supported inside MCM-41, we have demonstrated that the D,L-lactide polymerization occurs within the host channels to produce poly(D,L-lactide). More importantly, the characteristics of the resulting organic/inorganic polymer composite cannot be replicated by simple blending methods involving the polymer and MCM-41. This result, taken in combination with the spectroscopic, thermal, and surface volume measurements, indicates we can prepare a system where polymerization begins and propagates predominantly from inside the host channels. While contributions from trace chemistry occurring on the external surface of the crystallites cannot be excluded,[33] with our experimental preparation of the supported Sn catalyst, they are significantly minimized. Clear experimental evidence from a variety of methods, most notably solid-state NMR, indicate that polymer chains grow inside the channels and can only be removed by extensive washing with a good solvent. Mechanisms describing chemical interactions between the ring-opening catalyst and the host channel walls, as well as the subsequent polymerization steps, have been proposed based on experimental evidence. Future work will target optimized catalyst compositions, for example, different hosts and reduced Sn^{2+} concentrations, for higher molecular weight organic fractions in the composite.

Acknowledgment. The authors gratefully acknowledge support from the National Science Foundation through the Grants DMR-0611474 and DMR-0756291 and from the Oklahoma State Regents for Higher Education. A DuPont Science and Engineering Award (J.L.W.) provided additional research funding. Support for research instrumentation was provided by North Carolina State University and Oklahoma State University.

References and Notes

(1) Kresge, C. T.; Leonowicz, M. E.; Roth, W. J.; Vartuli, J. C.; Beck, J. S. *Nature* **1992**, *359*, 710.
(2) Zhao, D.; Feng, J.; Huo, Q.; Melosh, N.; Fredrickson, G. H.; Chmelka, B. F.; Stucky, G. D. *Science* **1998**, *279*, 548.
(3) Wight, A. P.; Davis, M. E. *Chem. Rev.* **2002**, *102*, 3589.
(4) Yang, K. K.; Wang, X. L.; Wang, Y. Z. *J. Ind. Eng. Chem.* **2007**, *13*, 485.
(5) Pandey, J. K.; Kumar, A. P.; Misra, M.; Mohanty, A. K.; Drzal, L. T.; Singh, R. P. *J. Nanosci. Nanotechnol.* **2005**, *5*, 497.
(6) Alexandre, M.; Dubois, P. *Mater. Sci. Eng.* **2000**, *28*, 1.
(7) Wu, D.; Zhang, Y.; Zhang, M.; Yu, W. *Biomacromolecules* **2009**, *10*, 417.
(8) Lv, G.; He, F.; Wang, X.; Gao, F.; Zhang, G.; Wang, T.; Jiang, H.; Wu, C.; Guo, D.; Li, X.; Chen, B.; Gu, Z. *Langmuir* **2008**, *24*, 2151.
(9) Thomassin, J. M.; Lou, X.; Pagnoulle, C.; Saib, A.; Bednarz, L.; Huynen, I.; Jerome, R.; Detrembleur, C. *J. Phys. Chem. C* **2007**, *111*, 11186.
(10) Pilla, S.; Gong, S.; O'neill, E.; Yang, L.; Rowell, R. M. *J. Appl. Polym. Sci.* **2009**, *111*, 37.
(11) Iovino, R.; Zullo, R.; Rao, M. A.; Cassar, L.; Gianfreda, L. *Polym. Degrad. Stab.* **2008**, *93*, 147.
(12) Jiang, L.; Morelius, E.; Zhang, J.; Wolcott, M. *J. Compos. Mater.* **2008**, *42*, 2629.
(13) Zhang, J.; Lou, J.; Ilias, S.; Krishnamachari, P.; Yan, J. *Polymer* **2008**, *49*, 2381.
(14) Moller, K.; Bein, T.; Fischer, R. X. *Chem. Mater.* **1998**, *10*, 1841.
(15) Alvaro, M.; Cardin, D. J.; Colquhoun, H. M.; Garcia, H.; Gilbert, A.; Lay, A. K.; Thorpe, J. H. *Chem. Mater.* **2005**, *17*, 2546.
(16) Spange, S.; Graser, A.; Muller, H.; Zimmerman, Y.; Rehak, P.; Jager, C.; Fuess, H.; Baehtz, C. *Chem. Mater.* **2001**, *13*, 3698.
(17) He, J.; Shen, Y.; Evans, D. G.; Duan, X. *Chem. Mater.* **2003**, *15*, 3894.
(18) He, J.; Shen, Y.; Evans, D. G.; Duan, X.; Howe, R. F. *J. Porous Mater.* **2002**, *9*, 49.
(19) Xu, L.; Nakajima, H.; Manias, E.; Krishnamoorti, R. *Macromolecules* **2009**, *42*, 3795.

(20) He, J.; Shen, Y.; Evans, D. G.; Duan, X. *Composites, Part A* **2006**, *37*, 379.
(21) Wang, N.; Li, M.; Zhang, J. *Mater. Lett.* **2005**, *59*, 2685.
(22) Kageyama, K.; Ogino, S.; Aida, T.; Tatsumi, T. *Macromolecules* **1998**, *31*, 4069.
(23) Korventausta, J.; Rosling, A.; Andersson, J.; Lind, A.; Linden, M.; Jokinen, M.; Yli-Urpo, A. *Key Eng. Mater* **2004**, *254−256*, 557.
(24) Sullivan, M. J.; Maciel, G. E. *Anal. Chem.* **1982**, *54*, 1615.
(25) Stejskal, E. O.; Schaefer, J.; Waugh, J. S. *J. Magn. Reson.* **1977**, *28*, 105.
(26) Zhao, X. S.; Lu, G. Q.; Hu, X. *Microporous Mesoporous Mater.* **2000**, *41*, 37.
(27) (a) Schwach, G.; Coudane, J.; Engel, R.; Vert, M. *Biomaterials* **2002**, *23*, 993. (b) Kricheldorf, H. R.; Kreiser-Saunders, I.; Stricker, A. *Macromolecules* **2000**, *33*, 702. (c) Kiremitci-Gumusderelioglu, M.; Deniz, G. *Turk. J. Chem.* **1999**, *23*, 153. (d) Hyon, S. H.; Jamshidi, K.; Ikada, Y. *Biomaterials* **1997**, *18*, 1503. (e) Schwach, G.; Coudane, J.; Engel, R.; Vert, M. *Polym. Bull.* **1994**, *32*, 617. (f) Gilding, D. K.; Reed, A. M. *Polymer* **1979**, *20*, 1459.
(28) Zhao, X. S.; Lu, G. Q.; Whittaker, A. K.; Millar, G. J.; Zhu, H. Y. *J. Phys. Chem. B* **1997**, *101*, 6525.
(29) Epping, J. D.; Chmelka, B. F. *Curr. Opin. Colloid Interface Sci.* **2006**, *11*, 81.
(30) Kageyama, K.; Ogino, S.; Aida, T. *Macromolecules* **1998**, *31*, 4069.
(31) Dechy-Cabaret, O.; Martin-Vaca, B.; Bourissou, D. *Chem. Rev.* **2004**, *104*, 6147.
(32) Albertsson, A.-C.; Varma, I. K. *Biomacromolecules*. **2003**, *4*, 1466.
(33) de Juan, F.; Ruiz-Hitzky, E. *Adv. Mater.* **2000**, *12*, 430.